Journal of Hazardous Materials 409 (2021) 124918

Contents lists available at ScienceDirect

Journal of Hazardous Materials

journal homepage: www.elsevier.com/locate/jhazmat

AC/DC magnetic device for safe medical use of potentially harmful magnetic nanocarriers

Mislav Mustapić [a,*], Zvonko Glumac [a], Marija Heffer [b], Milorad Zjalić [b], Ivan Prološčić [a], Mostafa Masud [c], Senka Blažetić [e], Ana Vuković [e], Motasim Billah [c,d], Aslam Khan [f], Suzana Šegota [g], Md Shahriar Al Hossain [c,d,**]

[a] Department of Physics, University of Osijek, 31000 Osijek, Croatia
[b] Department of Medical Biology and Genetics, Faculty of Medicine, JJ Strossmayer University of Osijek, J. Huttlera 4, 31000 Osijek, Croatia
[c] Australian Institute for Bioengineering and Nanotechnology, University of Queensland, St. Lucia, Brisbane, QLD 4067, Australia
[d] School of Mechanical and Mining Engineering, University of Queensland, St. Lucia, Brisbane, QLD 4067, Australia
[e] Department of Biology, J.J. Strossmayer University of Osijek, Ulica Cara Hadrijana 8A, 31000 Osijek, Croatia
[f] King Abdullah Institute for Nanotechnology, King Saud University, Riyadh 11451, Saudi Arabia
[g] Division of Physical Chemistry, Ruđer Bošković Institute, 10000 Zagreb, Croatia

ARTICLE INFO

Keywords:
Magnetic nanoparticles
Cytotoxicity
Enzyme activity
Oxidative stress

ABSTRACT

Continuing our previous research work on a drug delivery system based on combined AC/DC magnetic fields, we have developed a prototype AC/DC magnetic syringe device for stimulation of drug release from drug carriers, with the options of injecting/removing drug carriers. The porous Fe_3O_4 carrier, in a dose-dependent manner, causes acute oxidative damage and reduces the viability of differentiated SH-SY5Y human neuroblastoma cells, indicating the necessity for its removal once it reaches the therapeutic concentration at the target tissue. The working mechanism of the device consists of three simple steps. First, direct injection of the drug adsorbed on the surface of a carrier via a needle inserted into the targeted area. The second step is stimulation of drug release using a combination of AC magnetic field (a coil magnetised needle with AC current) and permanent magnets (DC magnetic lens outside of the body), and the third step is removal of the drug carriers from the injected area after the completion of drug release by magnetising the tip of the needle with DC current. Removing the drug carriers allows us to avoid possible acute and long term side effects of the drug carriers in the patient's body, as well as any potential response of the body to the drug carriers.

1. Introduction

In the last 30 years, different novel drug delivery systems have been developed for medical practice, with the main focus on cancer treatment (Cairns et al., 2006; Primo et al., 2007; Soppimath et al., 2001; Mura et al., 2013; Din et al., 2017; Patra et al., 2018), curing heart disease using drug-eluting stents (McGinty, 2014; Lee and Hernandez, 2018), and smart delivery via nano-carriers (Nakayama et al., 2015; Traitel et al., 2008). Furthermore, certain devices, such as skin transdermal patches (Prausnitz and Langer, 2008; Alkilani et al., 2015), therapeutic contact lenses (Zhang et al., 2004), and implants (Lyndon et al., 2014; Anderson and Davis, 2017), have been developed for drug delivery. Improved targeted drug delivery system (TDDS) should have several advantages over the traditional methods of cancer treatment (oral, intravenous) (Bhavsar and Amiji, 2007; Huang and Hainfield, 2013), such as high precision of tumour targeting, minimal nonspecific accumulation, minimum time of drug release, and reduced side effects. The next generation of TDDS should allow higher doses of drugs with potentially more "aggressive" substances, allowing treatment and full control of the eluting process. Furthermore the TDDS should be able to protect the drug from enzymatic degradation, antibodies, and different environmental factors, in addition to facilitating rapid reduction of treatment duration.

Administration of the correct dosage of a delivered drug, considering its toxicity, as well as the possible toxicity of the vehicle containing the drug, and the optimal duration of drug elution, can have a significant

* Corresponding author.
** Corresponding author at: Australian Institute for Bioengineering and Nanotechnology, University of Queensland, St. Lucia, Brisbane, QLD 4067, Australia.
E-mail addresses: mmustapic@fizika.unios.hr (M. Mustapić), md.hossain@uq.edu.au (M.S. Al Hossain).

https://doi.org/10.1016/j.jhazmat.2020.124918
Received 1 September 2020; Received in revised form 23 October 2020; Accepted 31 October 2020
Available online 31 December 2020

influence that is vital for the patient's health and the healing process. Thus, the success of therapy strongly depends on delivering the right amount of drug within a specific time. Drug carriers also could be prone to long-term retention in the human body through accumulating in different parts of human organs, including the liver, kidney, spleen, and lungs (Choi et al., 2007; Decuzzi et al., 2010; Wiemann et al., 2017; Valentini et al., 2019). Many studies have shown that, if accumulated NPs exist for a long period under physiological conditions, they can generate toxic products with negative side effects, such as oxidative stress, fibrosis, an inflammatory response (Bilyy et al., 2020), chemotaxis, genotoxicity, and cell death (Barna et al., 2013; Qu et al., 2012; Hamilton et al., 2012; Xia et al., 2013; Warheit and Donner, 2010; Simon-Deckers et al., 2008). Potentially iron based NPs, which can penetrate the blood-brain barrier, may further increase the iron disbalance typical for Alzheimer's and Parkinson's disease. (Wang et al., 2016; Liu et al., 2018; Honda et al., 2004).

Lack of a mechanism to remove NPs and prevent their accumulation during prolonged therapy can introduce health risks due to genotoxicity. The DNA that is damaged through chromosomal fragmentation, point mutations, and oxidative DNA adducts may initiate carcinogenesis (Meng et al., 2013).

Over the last twenty years, metal oxide NPs have appeared in many promising applications as a catalyst (Liao et al., 2020; Konnerth et al., 2020; Liao et al., 2018; Doustkhah et al., 2019), and in optical and photovoltaic devices (Chueh et al., 2019; Lee et al., 2019; Wang et al., 2018).

NPs application has particularly large potential in medicine, especially as a targeted drug carriers. Among different types of NPs iron oxides Fe_2O_3 (hematite), and Fe_3O_4 (magnetite) are the most widely used as sources, mostly due to their magnetic properties, negligible toxicity, simplicity of synthesis, and relatively high magnetization (Vangijzegem et al., 2019; Marcu et al., 2013; Reshmi et al., 2009; Tucek et al., 2006). In some research, Fe and Co pure metal NPs have been employed as a drug carriers, due to their having some advantages over iron oxides, such as better magnetic properties, high saturation magnetization, and high specific loss of power (Arias et al., 2009; Pouponneau et al., 2009). Besides the toxicology issue, a high magnetic moment is an essential property for magnetic carriers. The external magnetic field, which guides the carrier and triggers the drug release mechanism, has considerable limitations in deep tissues of the human body, since the magnetic field strength and field gradient both decrease exponentially with the distance from the surface of the magnet source. To avoid the human immune system, the drug carrier can be covered with various organic compounds, surfactants, and ligands to ensure invisibility and achieve better physical and chemical properties in interaction with living cells. Some complex structures of nano-carriers, such as core/shell structures, can provide higher stability against oxidation and acidic environments, although reducing the magnetic property.

In our previous work, we demonstrated the significant advantages of using AC/DC magnetic fields for drug release by the examples of dye (methyl blue) and flavonols (Mustapić et al., 2016; Šegota et al., 2019). We hypothesized that the carrier alone could have not only long-term, but also acute effects on non-targeted tissue, which we tested by 24-hour exposure of SH-SY5Y human neuroblastoma cells to different concentrations of Fe_3O_4 NPs. Based on different toxicity findings and our previous research, we have developed a novel device for drug delivery, which shares some similarities with the laparoscopic technique in medicine, but uses the advantages of combined AC/DC magnetic fields (magnetised syringe) for stimulation of drug release and removal of drug carriers from the human body.

2. Results and discussion

2.1. Biomedical aspects of Fe_3O_4 NPs as drug carrier

Porous Fe_3O_4 magnetic NPs were used on differentiated SH-SY5Y human neuroblastoma cells for testing their potential toxicity. According to our previous research (Mustapić et al., 2016) as-prepared Fe_3O_4 NPs have size (TEM; XRD) between 20 and 30 nm, and pore size around 5 nm, what makes them sufficiently small for use in human bloodstream (e.g. capillaries), and contrary large enough to maintain high magnetization for external magnet manipulation.

Most of the smart delivery drugs are focused on cancer treatment, but our intention was to determine the harmfulness of the NP carrier for the off-target tissue. In these experiments, we used a tumour cell line that was differentiated into mature neurons using retinoic acid as a growth factor. Mature neurons are an example of long-lived cells that are highly resistant to various types of damage (Garbarino et al., 2015).

The success of therapy depends on delivering the right amount of drug optimized to the amount of drug carrier, utilizing the drug at the target, and safely removing the free drug carrier from the surrounding tissue to avoid its spreading into the surrounding tissue. Bearing in mind that the device that we are going to develop will allow rather quick release of the drug – within 2 h – and the removal of residual NPs, we tested only the acute toxic effects (within 24 h) using three different concentrations of Fe_3O_4 NPs: 0.01, 0.1 and 1 mg/ml. A dose dependent internalization of Fe_3O_4 NPs in exposed cells was evaluated by Prussian blue staining (Fig. 1). Even at the lowest concentrations, NPs were not fully internalized, but rather formed agglomerates in the intercellular space. We can assume that these precipitates in real tissue would be the target of tissue macrophages, but also a long-term irritant that would stimulate the inflammatory response.

Fe_3O_4 NPs are already approved for clinical use, despite the fact that they are bioactive in themselves. Their accumulation in the cell triggers reactive oxygen species (ROS) production through different redox reactions (Adhikari et al., 2019), leading to oxidative stress and cell damage or apoptosis (Alberts et al., 2014). Also, Fe_3O_4 NPs lead to mitochondrial damage and mitochondrially-induced apoptosis by ROS-independent mechanisms (Peng et al., 2018). Because of this, their internalization in the target tissue, usually tumorous, is a desirable event, but not if it happens in the surrounding tissue. The target tissue has a certain nanoparticle binding capacity, and when it is exceeded, spillage occurs. After the destruction of target cells, when the capacity of macrophages in the tissue to remove cell debris is exceeded, NPs will accumulate in the intercellular space. In both cases, it will be advantageous to rely on the therapeutic effect of the delivered drug and remove the Fe_3O_4 NPs as drug carriers from the place of delivery.

The assumption that the accumulation of Fe_3O_4 NPs has a negative effect on cells was further tested by MTT assay, which estimates cell viability based on mitochondrial function (Fig. 2). 24 h exposure to Fe_3O_4 NPs in 0.01 mg/ml concentration had no significant acute effect on cell viability, but two higher concentrations were cytotoxic. Our data correlate with results of Wu et al. (2013), while the study of Xue et al. (2012) demonstrated that there was no cytotoxic effect on PC12 neuroblastoma cells, even at 0.5 mg/ml concentration and after 48 h of exposure. Undifferentiated tumour neuroblastoma lines were used in both studies, and, to the best of our knowledge, our study is the first attempt to determine the toxicity of Fe_3O_4 NPs in vitro on differentiated neurons. A study on a hepatoma cell line provided data that involved not just concentration and time, but also the correlation of Fe_3O_4 NP size to cytotoxicity (Xie et al., 2016).

Oxidative stress, characterized by excessive production of reactive oxygen species (ROS), plays a great role in cellular viability. To remove ROS and reduce its toxic effects, cells evoke an antioxidant response through different antioxidant enzymes. In this study, the elicited antioxidant response was measured by catalase (CAT), superoxide dismutase (SOD), glutathione S-transferase (GST), and glutathione reductase (GR)

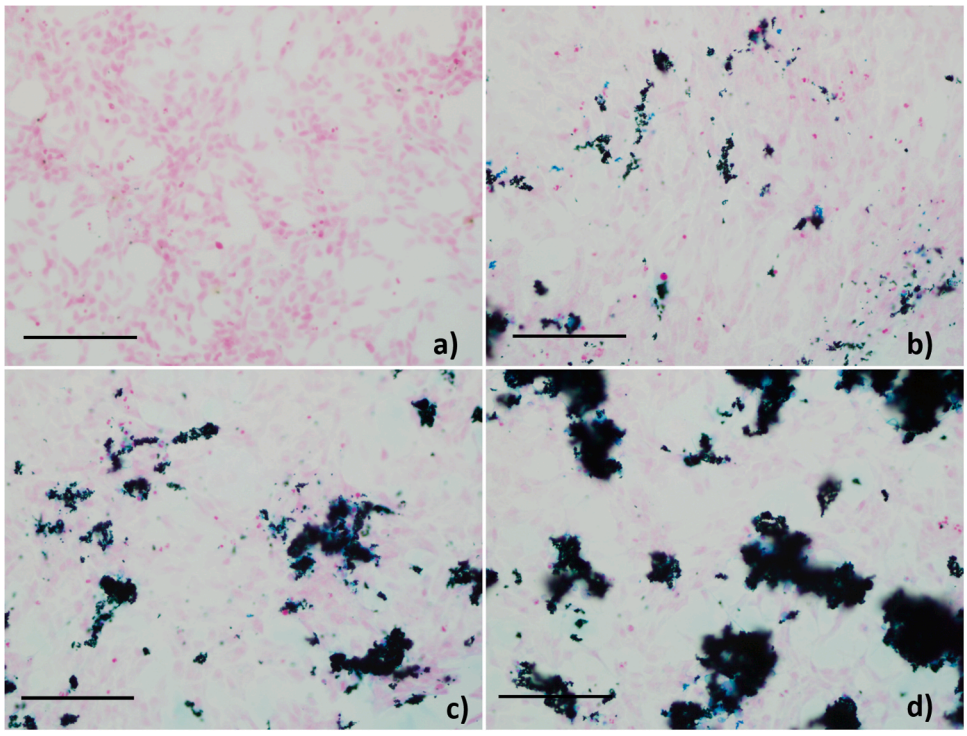

Fig. 1. Prussian blue staining against iron on differentiated SH-SY5Y human neuroblastoma cell line at 24 h post exposure to different concentrations of Fe_3O_4 nanoparticles; A – 0 mg/ml (control), B – 0.01 mg/ml, C – 0.1 mg/ml, D – 1 mg/ml; Blue – metabolised iron positive stain, Red – nuclei and cytoplasm, Black – non metabolised nanoparticles; magnification 400 × ; Scale 100 μm. (For interpretation of the references to colour in this figure legend, the reader is referred to the web version of this article).

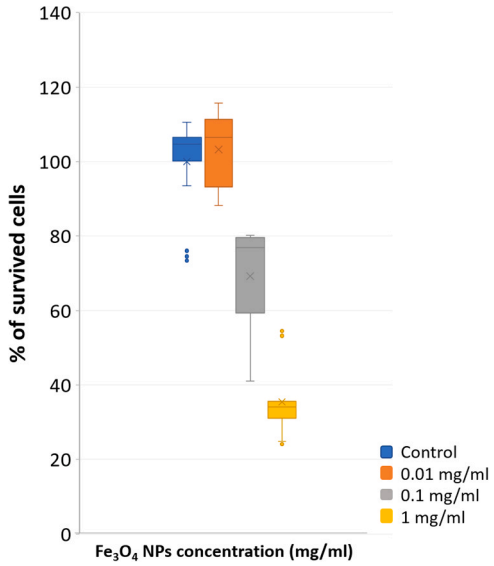

Fig. 2. MTT viability assay on differentiated SH-SY5Y human neuroblastoma cell line 24 h post exposure to Fe_3O_4 nanoparticles. Statistical analysis by Kruskal-Wallis with Dunn post hoc and correction for number of groups was used, $^*p < 0.05$, $^{**}p < 0.01$, $^{***}p < 0.001$ in Statistica 13.3.

enzyme activity. According to the results, short term exposure of neuroblastoma cells to a 0.01 mg/ml concentration of Fe_3O_4 NPs did not evoke a significant response to oxidative stress at the level of all analysed enzymes (Fig. 3). CAT and SOD showed a significant increase only at 1 mg/ml concentration, while GST and GR were more sensitive to the presence of Fe_3O_4 NPs and showed significantly increased activity at lower concentration (0.1 mg/ml). GST and GR are likely to be part of the "first line" of biochemical response to oxidative stress in neuroblastoma cells.

Gambardella et al. (2014), in their study on *Artemia salina* larvae, found significantly increased CAT activity, even after exposure to the lowest dose of Fe_3O_4 NPs used in our study. The possible reasons for this difference in the oxidative stress response lies in the fact that differentiated neurons are more resistant to oxidative stress than any other type of eukaryotic cell. Özgür et al. (2018) found a decrease in CAT and SOD activity in rainbow trout sperm exposed to doses of 0.1–0.8 mg/ml Fe_3O_4 NPs, which could be due to excessive ROS production in these cells.

We also measured the production of malondialdehyde (MDA) which reflects oxidative damage to lipids in the form of lipid peroxidation (Fig. 4). MDA concentrations were significantly increased from Fe_3O_4 NPs from the concentration of 0.1 mg/ml. Our results are further confirmation of the results obtained on skin epithelial cells and a pulmonary epithelial cell line, where Fe_3O_4 NPs were found to cause an increase in oxidative stress and lipid peroxidation in exposed cells (Ahamed et al., 2013). The negative effect of Fe_3O_4 NPs on differentiated neuroblastoma cells is due to instability and easy oxidation, yielding γ-$Fe_2O_3 + Fe^{2+}$ (Singh et al., 2010).

The role of the biochemical response to oxidative stress is to protect the cell from irreparable damage. If the damage exceeds the capacity of the antioxidant defence mechanisms, programmed cell death (apoptosis) is triggered. The number of apoptotic cells was detected by the TUNEL assay showing DNA fragmentation. A significant number of apoptotic cells appeared only at an Fe_3O_4 NP concentration of 1 mg/ml (Fig. 5), while lower concentrations of NPs raise cellular defence mechanisms that can protect them against permanent damage and death. In complex biological systems, it would be desirable to prevent damaging concentrations of particles, which is characteristic of organs that excrete substances from the body – the kidney and the liver.

Since we were working on a model of mature neurons, our next question was whether oxidative damage and non-oxidation-related nanoparticle-induced neuronal damage would lead to a predisposition to neurodegeneration. Disruption of iron homeostasis was previously connected with neurodegenerative disorders (Hautot et al., 2003; Wu et al., 2013).

We decided to investigate the expression of beta amyloid precursor protein (βAPP) and GM1 ganglioside due to their role in the pathogenesis of Alzheimer's disease (AD) (Liu et al., 2006). Short term exposure

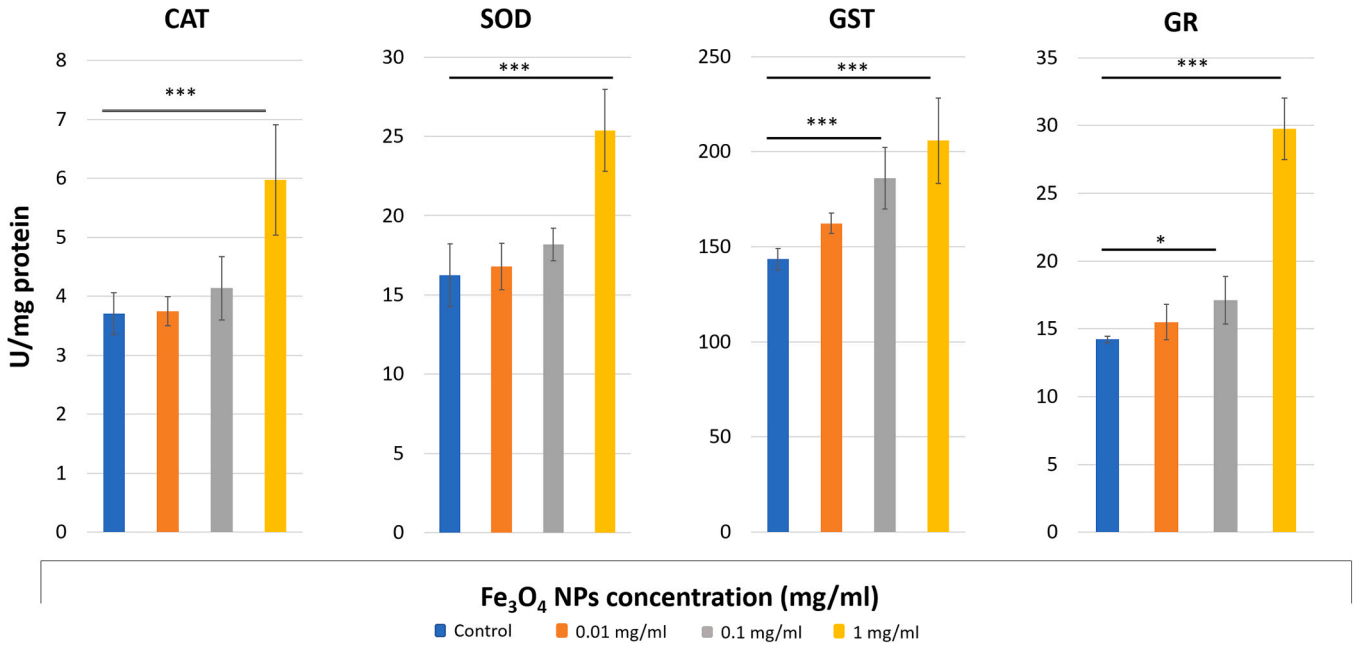

Fig. 3. Antioxidant enzyme activity assay (E) on differentiated SH-SY5Y human neuroblastoma cell line 24 h post exposure to Fe_3O_4 nanoparticles presented as mean with standard deviation (SD). Differences among groups were assessed by a one-way analysis of variance (ANOVA), followed by a post hoc analysis using the Tukey HSD test. Correlations between the analysed parameters were evaluated using the Pearson correlation coefficient with the level of significance < 0.05. *$p < 0.05$, ** $p < 0.01$, *** $p < 0.001$ in Statistica 13.3. Abbreviations on y-axis labels: catalase (CAT), superoxide dismutase (SOD), glutathione S-transferase (GST), and glutathione reductase (GR).

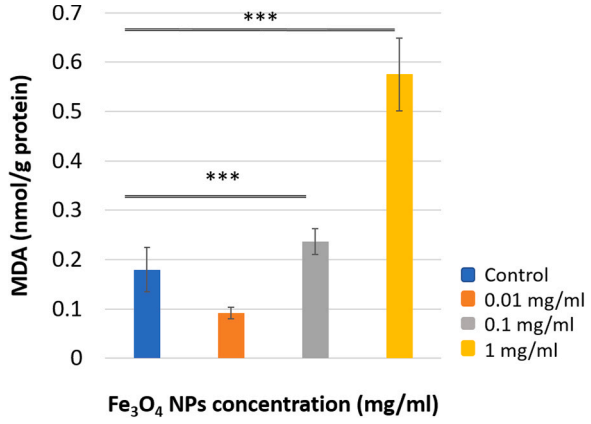

Fig. 4. Lipid peroxidation on differentiated SH-SY5Y human neuroblastoma cell line 24 h post exposure to Fe_3O_4 nanoparticles presented as mean with standard deviation (SD). Differences among groups were assessed by a one-way analysis of variance (ANOVA), followed by a post hoc analysis using the Tukey HSD test. Correlations between the analysed parameters were evaluated using the Pearson correlation coefficient with the level of significance < 0.05. *$p < 0.05$, ** $p < 0.01$, *** $p < 0.001$ in Statistica 13.3.

to even the smallest concentration of Fe_3O_4 NPs caused a decrease in GM1 expression, while just the highest concentration of Fe_3O_4 NPs (1 mg/ml) caused significant accumulation of βAPP as the hallmark of neurodegeneration (Fig. 6). Earlier studies assumed that GM1 played a role in amyloid precipitation (Tashima et al., 2004; Yanagisawa and Ihara, 1998), but more recent studies tell the opposite – GM1 is neuroprotective against Aβ-induced toxicity (Cebecauer et al., 2017) and promotes neurite formation in neuroblastoma cells (Chiricozzi et al., 2017). If we associate the decrease in GM1 with the increased production of βAPP, one can assume that neurons exposed to Fe_3O_4 NPs showed an increased risk of Aβ precipitation and decreased potential for new dendrites to form, that is, they acquired a pre-degeneration phenotype.

2.2. Novel concept idea

The AC/DC magnetic setup represents a simple and efficient targeted drug delivery system, while it also makes it possible to remove the drug carriers from the body after treatment. The AC/DC magnetic set-up is made up of three main parts: 1) a syringe and needle made in one piece from permalloy (easy to magnetize and very small coercive field), with a coil wrapped around the body of syringe, as shown in Fig. 7a, b; 2) a source of alternating electrical current (signal generator) connected to the coil (Fig. 7b); and 3) a set of permanent magnets fixed on an adjustable half-ring (Fig. 8). The basic set-up can have some additional supporting parts, such as a current amplifier to increase the electrical current in the coil and improve the magnetization of the syringe and needle.

In principle, magnetic carriers with loaded drugs will be injected into the targeted area using the magnetic syringe without applying AC current. The length of the needle will ensure access to different parts of the human body. Strong external permanent magnets will steer the magnetic NPs into the targeted area (acting as a magnetic lens) and promote the drug elution by creating oscillating filaments (video). According to our previous research, oscillation of the magnetic NPs (filaments due to alignment in the DC field) will produce friction between the NPs, as well as between the particles and the tissue or body fluids, and consequently release the drug (classical Brownian motion) (Šegota et al., 2019; Kramers, 1940).

As we have demonstrated before, the power of AC/DC magnetic fields depends on the distance from the magnetic NPs (carriers) (videos 1, 2, 3, 4). It can be seen that, even at a distance of 5 cm, it is still possible to see the movement (oscillation) of magnetic particles. It is important to emphasize that, in all experiments, we used a current of 100 mA and permanent magnets with magnetic fields of ~ 500–1000 Oe, which can be characterized as weak magnetic fields.

Supplementary material related to this article can be found online at doi:10.1016/j.jhazmat.2020.124918.

Applying both magnetic AC and DC fields will ensure precise and efficient release of the drug from the magnetic carriers into the area of

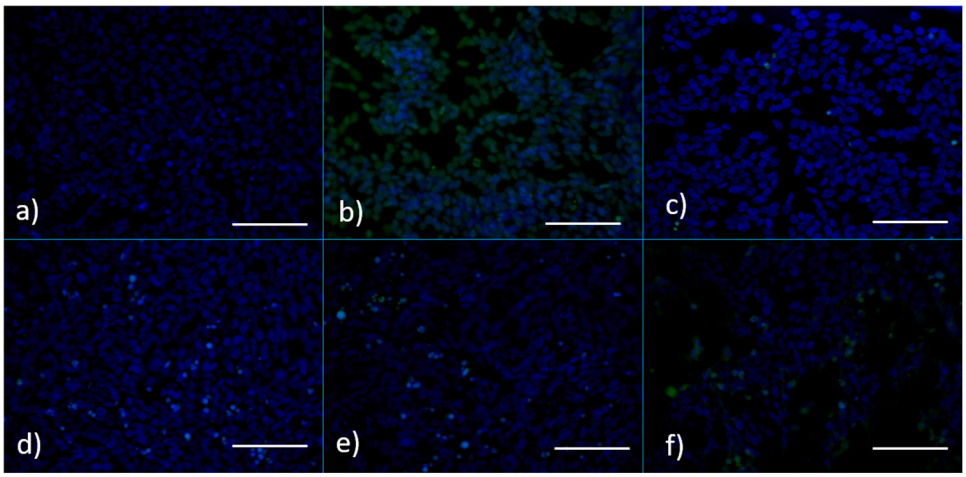

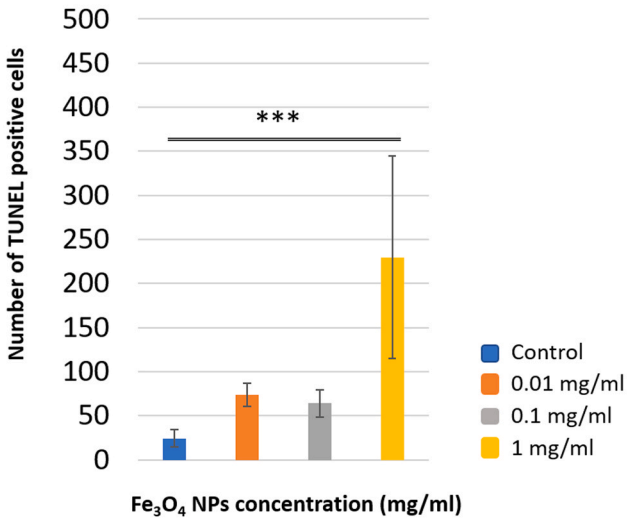

Fig. 5. TUNEL assay against single strand DNA breakage on differentiated SH-SY5Y human neuroblastoma cell line after 24 h post exposure to Fe_3O_4 nanoparticles. Upper image: A – negative stain control, B – positive stain control, C – 0 mg/ml of Fe_3O_4 nanoparticles, D – 0.01 mg/ml of Fe_3O_4 nanoparticles, E – 0.1 mg/ml of Fe_3O_4 nanoparticles, F – 1 mg/ml of Fe_3O_4 nanoparticles; Blue – 4′,6-diamidino-2-phenylindole (DAPI) stained nuclei, Green – TUNEL assay fluorescein (FITC) positive signal; magnification 400 ×; Scale 100 μm. Graph: Number of TUNEL positive cells presented as mean with SD against single strand DNA breakage. Statistical analysis was conducted using ANOVA with post-hoc Tukey HSD; * $p < 0.05$, ** $p < 0.01$, *** $p < 0.001$ in Statistica 13.3. (For interpretation of the references to colour in this figure legend, the reader is referred to the web version of this article).

the tumour with a controlled rate of drug elution, simply by changing the frequency of the AC current. After treatment, the AC current power supply will be shut down, and the magnetic carriers will be removed using the highly magnetized syringe and DC current (video 5). The removed magnetic carriers can be reused for the next treatment after cleaning and sterilisation.

Supplementary material related to this article can be found online at doi:10.1016/j.jhazmat.2020.124918.

In practice, to efficiently treat tumor tissue deeper in the human body by magnetic field presents a problem due to the considerable decrease in strength of the magnetic field with distance (r^{-2}). Unregulated growth of tumour vasculature also will affect the high pressure in the bloodstream, leading to some limitations on the generation of a high magnetic field. Therefore, the distribution of blood vessels across cancer tissue leads to the formation of patches, some with very high blood supply and others with almost negligible supply (Forster et al., 2017; Nagy et al., 2009). Direct injection into the tumour area will avoid the bloodstream and all possible complications related to the body enzymes, antibodies, irregular blood pressure, and slow elution of drugs during delivery. One well known example of a barrier in the human body is the brain blood barrier (BBB), which can strongly obstruct any medical treatment in the brain. Some iron based NPs are able to cross BBB, but the use of the magnetic syringe will further help to overcome the BBB and efficiently release the drug in the targeted area.

Although some drug carriers, such as Fe_3O_4 (Nakayama et al., 2015; Qi et al., 2016; Nagy et al., 2009; Shen et al., 2018; El-Boubbou, 2018), have received clinical approval, accumulation of all kinds of NPs can create potential side effects, especially over an extended period. Intravenous injection of a drug may lead to several problems, such as degradation of the drug by enzymes or the immune system in the human body. Furthermore, with our proposed device, the drug can be released into a targeted small area, and the controlled rate of drug release will prevent the possible spillover of medicine into a much larger area than the specific targeted area. Two research groups have suggested application of a simple magnetic needle to attract magnetic NPs used for medical purposes (Ramaswamy et al., 2015; Bryant et al., 2007).

2.3. Drug release profile

We performed our experiments on normal drug (myricitrin) release in three different situation, first without any magnetic field (no magnet), second with applied external permanent magnetic field, and third with combined permanent and oscillating magnetic fields (8 Hz) AC/DC. As a drug sample we used the flavonoid myricitrin from our previous research (Šegota et al., 2019). The cumulative profile of drug release under three different conditions is shown in Fig. 9.

The first condition of drug release from Fe_3O_4 NPs was with no magnetic field. The drug (myricitrin) release rate was initially moderate and became slower with time. Briefly, after 50 h, slightly over 50% of drug was released, and after 220 h all of the drug was released. The second condition for the drug (myricitrin) release profile was under a permanent magnetic field (Fig. 9). The experimental data show a very similar curve of drug release compared to the first condition with no magnet. The amounts of drug release under the permanent magnet are

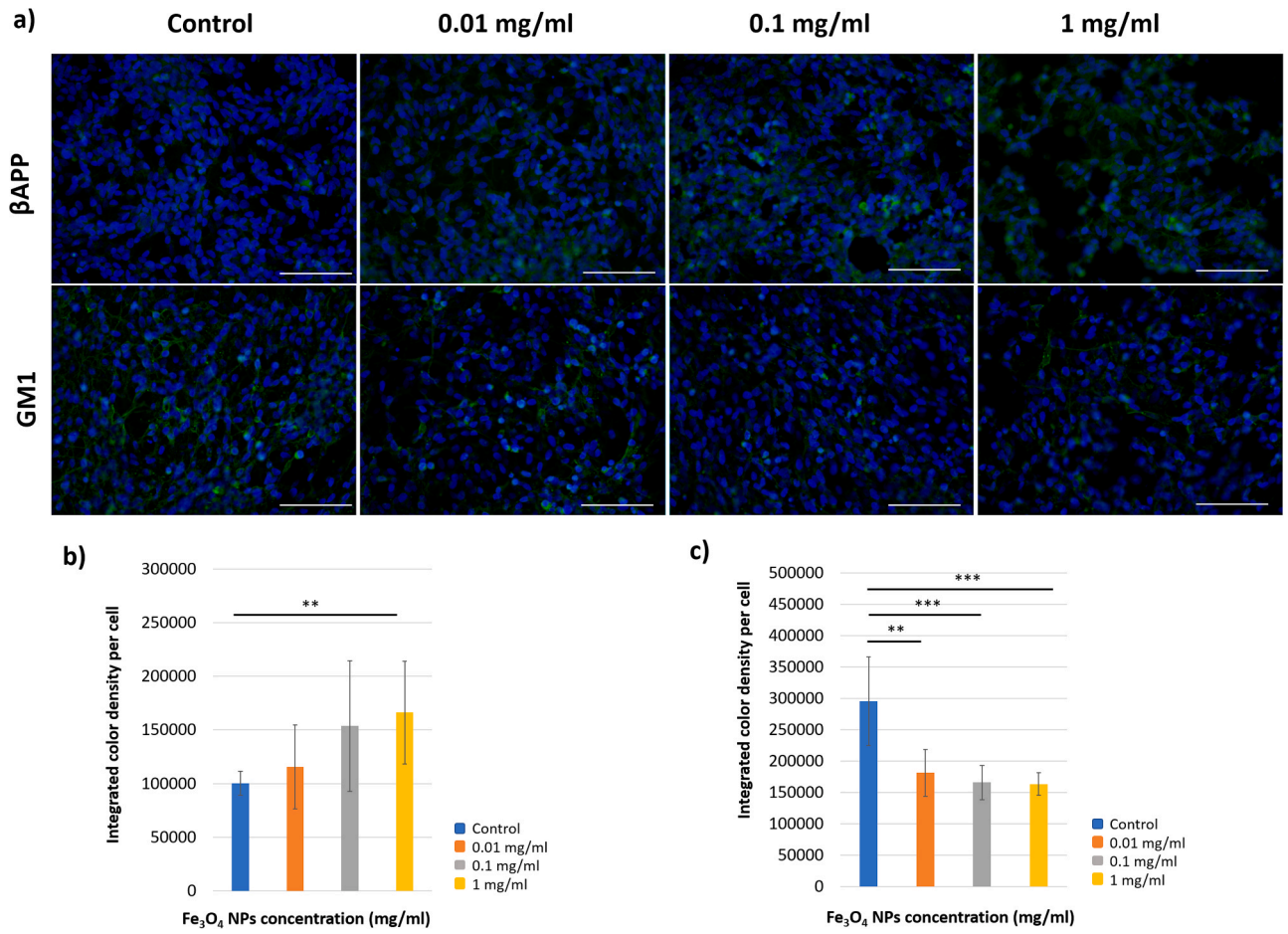

Fig. 6. (a) Immunoreactivity of differentiated SH-SY5Y human neuroblastoma cell line toward βAPP and GM1 24 h post exposure to different concentration of Fe_3O_4 nanoparticles. (a) Immunocytochemical staining against βAPP and GM1; Blue – DAPI stained nuclei, Green – βAPP and GM1 positive signal; magnification 400 × ; Scale 100 μm. Quantification of βAPP (b) and GM1 (c) staining. Statistical analysis was conducted using ANOVA with post-hoc Tukey HSD; * $p < 0.05$, ** $p < 0.01$, *** $p < 0.001$ in Statistica 13.3. (For interpretation of the references to colour in this figure legend, the reader is referred to the web version of this article).

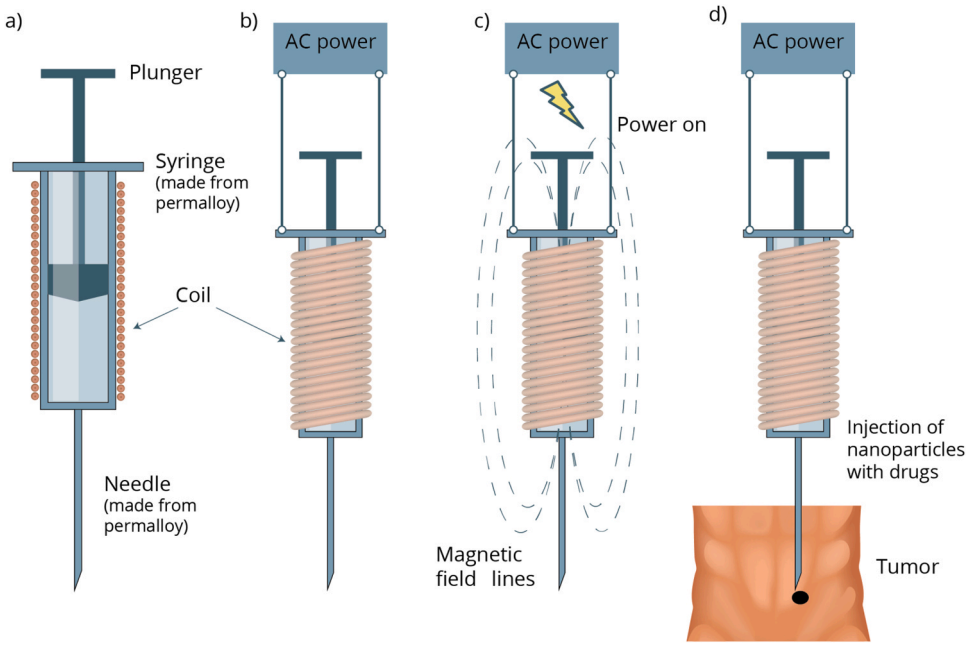

Fig. 7. Construction and principles of AC/DC magnetic syringe device: (a) and (b) Main parts of the AC/DC magnetic syringe device. (c) Lines of magnetic flux after applying AC current in the coil. (d) Injection of drug carriers into the tumor area without applying an AC magnetic field.

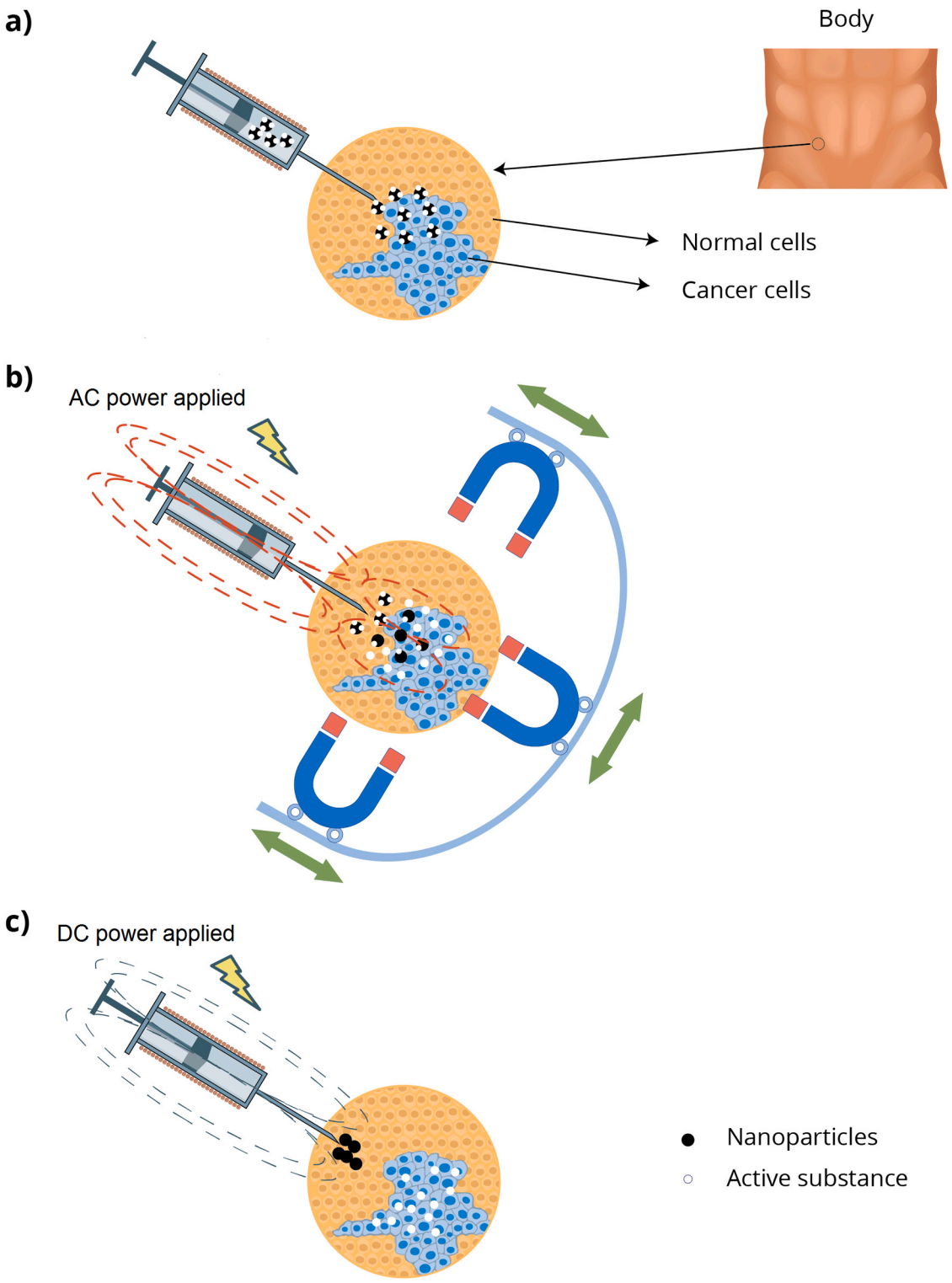

Fig. 8. Full set-up of the AC/DC magnetic syringe device with external permanent magnets for focusing the magnetic field (magnetic lens). Method of application: (a) injection of Fe_3O_4 nanoparticles with active substance, (b) releasing active substance from Fe_3O_4 nanoparticles with applying AC/DC magnetic fields (c) removing Fe_3O_4 nanoparticles from targeted area.

slightly lower after 50 and 150 h. Just as in the measurement with no magnet, all of the drug was released after 220 h.

On the contrary, the release rate increased dramatically when drug carriers (Fe_3O_4 NPs) were exposed to a combined permanent and oscillating AC/DC magnetic field (8 Hz). All of the drug was released within 2 h, which is more than 100 times faster in comparison to drug release with no magnet or with only permanent magnet conditions. These results are in very good agreement with our previous research (Šegota et al., 2019), and open up new possibilities for more efficient and precise drug delivery.

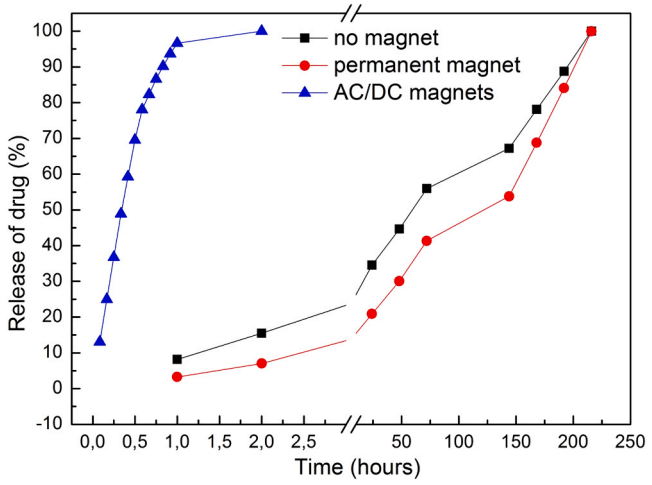

Fig. 9. Cumulative release profiles of drug (myricitrin) from nanoparticles with no magnetic field applied, permanent magnetic field, and AC/DC magnetic fields.

2.4. Influence of the combined magnetic fields (AC/DC) on magnetic nanocarriers injected into a targeted area (fluid)

Magnetic nanoparticles are exposed to a magnetic field, $\vec{B}$ which is a combination of a static field $\vec{B_s}$ and an oscillating field, $\vec{B_{os}}$. The fields are perpendicular to each other:

$$\vec{B} = \vec{B}_s + \vec{B}_{os} = B_s(\vec{r})\,\vec{e}_x + B_{os,0}(\vec{r})\cos(\omega_H t)\,\vec{e}_y \tag{1}$$

where ω_H is the radial frequency of the oscillating magnetic field, and t is time.

Both fields induce magnetic dipole moments

$$\vec{m}_s = V\chi\,\vec{B}_s, \quad \vec{m}_{os} = V\chi\,\vec{B}_{os}, \tag{2}$$

where V is the volume of the particles, and χ is the magnetic susceptibility.

The static field $\vec{B_s}$ is important because the superparamagnetic NPs do not have a significant magnetic moment in zero field (since they are randomly oriented due to the thermal excitation), and their net magnetization is zero. When only a static magnetic field is applied, the magnetic moment $\vec{m_s}$ of single-domain particles will align in the direction of the static magnetic field (easy axis), minimising the static potential energy.

The filaments are thus aligned NPs (quite analogous to the situation where the shape of the magnetic field produced by a permanent magnet is revealed by the orientation of iron filings). They are formed only if the stationary field is turned on and is strong and inhomogeneous enough to move the aggregated NPs, having on average a diameter, $2R$, of a few hundreds of nanometers, through the viscous fluid and ensure a transition into a more ordered state. The equilibrium is reached because of the boundary conditions (gravity).

With only the permanent field present, there is no force to move an aggregate away from its equilibrium position. By applying the oscillating magnetic field $\vec{B_{os}}$, when the filaments have been formed, the movement of aggregates is significantly intensified. The amplitude and velocity of oscillation around the easy axis depends on the frequency of the oscillating field ω_H (videos 1–5). From the video, it can be seen that the motion (swinging) of the magnetic filaments (i.e. NP aggregates in the flux of a static magnetic field) is controlled by the combined static/oscillating magnetic fields in the fluid (water) (Mustapić et al., 2016; Šegota et al., 2019).

It follows that the two main forces acting on the NPs in the fluid are the force of the nonhomogenous oscillating magnetic field,

$$\vec{F}_{os} = \vec{\nabla}(\vec{m}_{os}\cdot\vec{B}_{os}) \tag{3}$$

and the Stoke's drag force representing the frictional drag force moving the particles in a viscous fluid

$$\vec{F}_{St} = -6\,\pi\,\eta\,R\,\vec{v}_p, \tag{4}$$

where, R is the radius of the particles, η is the viscosity of the fluid, and $\vec{v_p}$ is the velocity of the particles. Hence, the motion of the NPs is derived from the following equation (Wei et al., 2019):

$$m_p\frac{d\vec{v}_p}{dt} = \vec{\nabla}(\vec{m}_{os}\cdot\vec{B}_{os}) - 6\pi\eta R\vec{v}_p, \tag{5}$$

where m_p is the mass of the particles and $\vec{v_p}$ is the velocity of the particles.

The oscillating field causes constant collisions and friction with the molecules of water, and can be the main factor behind the quicker and smoother release of the drug molecules from the interior of the NPs (Wei and Wang, 2018).

2.5. The induced magnetic field of a coil with finite dimensions

In this experiment, we used a standard coil with current $I = 100$ mA, and the dimensional parameters of the inner radius of the coil, $R_U = 0.4$ cm, and the outer radius, $R_V = 0.6$ cm. The length of the coil is $L = 6.5$ cm, and number of turns $N = 1000$. The induction of the magnetic field, $\vec{B}$, was calculated by Biot-Savart's law. The standard calculation leads to an expression for $\vec{B}$ at any point $\vec{e}_z$ on the symmetry axis of the coil:

$$\vec{\mathbf{B}}(z,t) = \vec{\mathbf{e}}_z\frac{\mu_o N\,I(t)}{2L(R_v-R_u)}\left[\left(z+\frac{L}{2}\right)\ln\frac{R_v+\sqrt{R_v^2+(z+\frac{L}{2})^2}}{R_u+\sqrt{R_u^2+(z+\frac{L}{2})^2}} - \left(z-\frac{L}{2}\right)\ln\frac{R_v+\sqrt{R_v^2+(z-\frac{L}{2})^2}}{R_u+\sqrt{R_u^2+(z-\frac{L}{2})^2}}\right]. \tag{6}$$

Fig. 10(a) shows the induction of a magnetic field $\vec{B}$ scaled by the characteristic field $B_0 = (\mu_0 NI)/[2(R_V\text{-}R_U)]$. The field $\vec{B}$ is symmetric according to the (x,y) plane:

$$B(z) = B(-z). \tag{7}$$

In the case of a DC current I (steady current flow through the coil), the $\vec{B}$ field will have a certain value for a particular point in the space z. On the other hand, for the AC current $I(t) = I_0 cos\ (\omega_H\, t)$ at a particular point z, the $\vec{B}$ field changes with time from $+\vec{B}$ to $-\vec{B}$.

In the example of a magnetic dipole with constant value $m_o > 0$ and with a certain direction $\vec{e}_r$

$$\vec{m} = m_0\,\vec{e}_r. \tag{8}$$

The potential energy of the dipole in the external magnetic field $\vec{B}$ is equal to:

$$E_p = -\vec{\mathbf{m}}\cdot\vec{\mathbf{B}} \tag{9}$$

and the force on it is the negative gradient of the potential energy:

$$\vec{\mathbf{F}}_B = \vec{\nabla}\left(\vec{\mathbf{m}}\cdot\vec{\mathbf{B}}\right) = \vec{\mathbf{e}}_z m_0\cos(\theta)\frac{\partial B}{\partial z}. \tag{10}$$

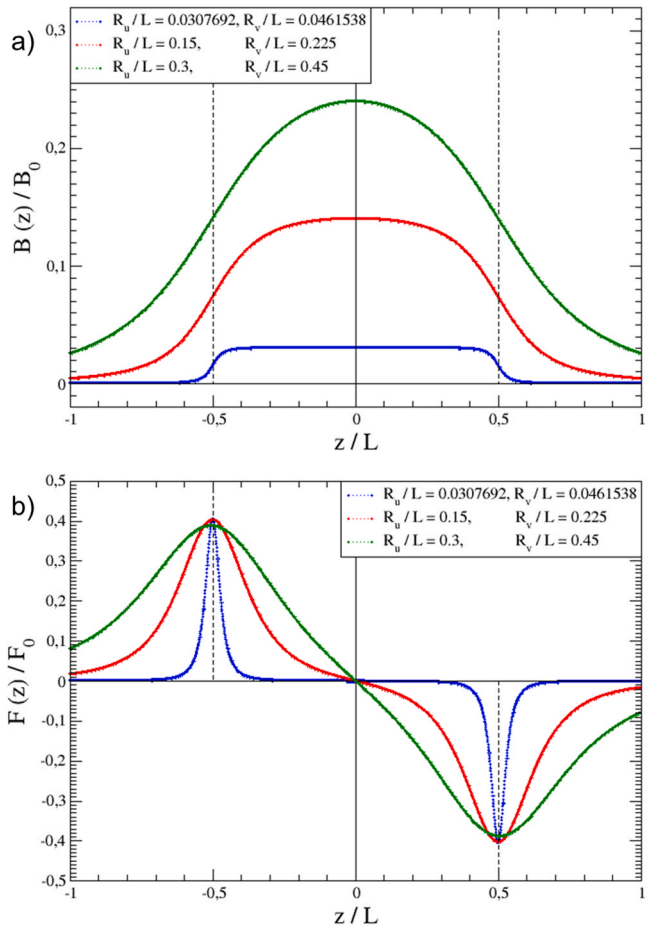

Fig. 10. Dependence of the ratios $B_{(z)}/B_0$ (a), and $F_{(z)}/F_0$ (b) as functions of the dimensionless ratio z/L for several values of R_U/L and R_V/L. The dotted lines represent the edges of the coil at points $z = \pm L/2$.

$$\vec{\mathbf{F}}_B = \vec{\mathbf{e}}_z F_0 \left\{ \ln \left[\frac{R_v + \sqrt{R_v^2 + (z+\frac{L}{2})^2}}{R_u + \sqrt{R_u^2 + (z+\frac{L}{2})^2}} \frac{R_u + \sqrt{R_u^2 + (z+\frac{L}{2})^2}}{R_v + \sqrt{R_v^2 + (z+\frac{L}{2})^2}} \right] + \left(z+\frac{L}{2}\right)^2 \frac{\phi_1(+)}{\phi_2(+)} + \left(z-\frac{L}{2}\right)^2 \frac{\phi_1(-)}{\phi_2(-)} \right\}, \quad (11)$$

where,

$$F_0 = \frac{\mu_0 m_0 \cos(\theta) N\, I(t)}{2L(R_v - R_u)},$$

$$\phi_1(\pm) = R_u \left(R_u + \sqrt{R_u^2 + (z \pm \tfrac{L}{2})^2} \right) - R_v \left(R_v + \sqrt{R_v^2 + (z \pm \tfrac{L}{2})^2} \right),$$

$$\phi_2(\pm) = \sqrt{R_u^2 + (z \pm \tfrac{L}{2})^2} \cdot \sqrt{R_v^2 + \left(z \pm \tfrac{L}{2}\right)^2} \cdot \left(R_u + \sqrt{R_u^2 + (z \pm \tfrac{L}{2})^2} \right) \cdot \left(R_v + \sqrt{R_v^2 + (z \pm \tfrac{L}{2})^2} \right).$$

$\boldsymbol{F}(z)$ is shown on the right side of Fig. 10(b) scaled by the characteristic force F_0. The graph shows that the force is the greatest on the edge of the coil and then starts to decreases with distance from the edge. The decline is slower if the coil is thicker. In the case of direct current, the force will have the same value at the same point of space z. In contrast, for alternating current $I(t) = I_0 cos\ (\omega_H t)$, the value of $\vec{F}(z,t)$ at every point z will change with time from value of $-\vec{F}$ to $+\vec{F}$, and the force will cause a change in the magnetic dipole direction.

3. Conclusion

To summarize, our AC/DC magnetic syringe device represents a simple and efficient targeted drug delivery device with multiple functions. This concept is just at a very early stage, but it has high potential for clinical use in the near future, not only for drug delivery, but also for imaging or for removing unwanted substances from the human body (opposite direction). The magnetised syringe provides an efficient means of targeted drug delivery, even for remote parts of the human body, with significant potential for upgrading by including a camera. Even though the possible toxic effects of different NPs, including Fe_3O_4 NPs, have been previously known and are confirmed by this study, the possibility of removing NPs once they have performed their function and delivered the active substance to the target tissue has still not been considered. The negative effects of Fe_3O_4 NPs, based on all measured parameters, are dose dependent and acute. This is why the AC/DC magnetic syringe has an advantage - it offers the possibility of removing Fe_3O_4 NPs after drug release, which greatly reduces the cytotoxic effect of the carrier.

This concept represents the very early stage of one promising TDD system, and additional research will have to be undertaken, especially pre-clinical research (living animals), as well as solving the problems of obtaining the most efficient technical design of the device itself.

Finally, we provide a list of advantages of our new drug delivery device:

1) Constructed as one part, the coil and syringe can be designed with different dimensions and lengths, with possible upgrades (e.g. a camera) following demand.
2) The drug can be released directly into the tumour area, avoiding the bloodstream and other barriers in human body, and can be immediately triggered by applying AC/DC magnetic fields.
3) Magnetic flux in the needle tip will make a sufficiently strong magnetic field gradient to manipulate NPs (oscillation), even in remote parts of the human body.
4) Direct manipulation of the strength of the magnetic fields (AC and DC) is possible, as is obtaining an accurate rate of drug elution by adjusting the frequency of the AC magnetic field.
5) Permanent magnets will be used for precisely focusing NPs on the targeted area and for increasing drug release (filaments), as well as finally providing for safe removal of the nanoparticles from the human body.
6) An additional possibility for the AC/DC magnetic syringe device is, for example, the removal of unhealthy substances from the human body using high potential for adsorption on the large specific surface area of nanomaterials.
7) A high concentration of magnetic particles can be introduced into targeted parts of the human body for nuclear magnetic resonance (NMR) imaging and later safely removed after the imaging session.
8) The additional option of removing the magnetic material provides the possibility of using more “aggressive” (i.e. toxic) substances for clinical use.

CRediT authorship contribution statement

Mislav Mustapić: Experiment and device design, performing experiments, data interpretation, writing original manuscript, Reviewing and Editing. **Zvonko Glumac**: Data interpretation, writing a section of manuscript. **Marija Heffer**: Performing experiments, data interpretation, writing some parts of manuscript. **Milorad Zjalić**: Performing experiments, data interpretation. **Ivan Prološčić**: performing experiment. **Mostafa Masud**: Reviewing and editing. **Senka Blažetić**: Performing

experiments, data interpretation. **Ana Vuković**: Performing experiments, data interpretation. **Motasim Billah**: Performing experiments. **Aslam Khan**: Reviewing and Editing. **Suzana Šegota**: Performing experiments, data interpretation. **Md. Shahriar A. Hossain**: Data interpretation, writing original manuscript, Reviewing and Editing.

Declaration of Competing Interest

The authors declare that they have no known competing financial interests or personal relationships that could have appeared to influence the work reported in this paper.

Acknowledgements

This work has been supported by an internal funding project of the Josip Juraj Strossmayer University of Osijek (ZUP-2018-56), and the Australian Research Council (Grant No. LP160101784). This work was partially supported by the Researchers Supporting Project (No. RSP-2021/127), King Saud University, Riyadh, Saudi Arabia. This work was performed in part at the Queensland node of the Australian National Fabrication Facility (ANFF), a company established under the National Collaborative Research Infrastructure Strategy to provide nano and microfabrication facilities for Australian researchers.

This work has also been supported by the Croatian Science Foundation (Croatia) under the projects IP-2014-09-2324 (foundation grant to MH) and IP-2016-06-8415 (foundation grant to SŠ), and by the European Union through the European Regional Development Fund, Operational Programme Competitiveness and Cohesion (grant agreement No. KK.01.1.1.01.0007, CoRE - Neuro, Croatia). MM thanks Tomislav Čorak for graphical design.

Appendix A. Supporting information

Supplementary data associated with this article can be found in the online version at doi:10.1016/j.jhazmat.2020.124918.

References

Adhikari, A., Mondal, S., Darbar, S., Kumar Pal, S., 2019. Role of nanomedicine in redox mediated healing at molecular level. Biomol. Concepts 10, 160–174. https://doi.org/10.1515/bmc-2019-0019.

Ahamed, M., Alhadlaq, H.A., Alam, J., Majeed Khan, M.A., Ali, D., Alarafi, S., 2013. Iron oxide nanoparticle-induced oxidative stress and genotoxicity in human skin epithelial and lung epithelial cell lines. Curr. Pharm. Des. 19, 6681–6690. https://doi.org/10.2174/1381612811319370011.

Alberts, B., Johnson, A., Lewis, J., Morgan, D., Raff, M., Roberts, K., Walter, P., 2014. Molecular Biology of the Cell, 6th ed...,. Garland Science,, New York, p. 1025.

Alkilani, A.Z., McCrudden, M.T.C., Donnelly, R.F., 2015. Transdermal drug delivery: innovative pharmaceutical developments based on disruption of the barrier properties of the stratum corneum. Pharmaceutics 7, 438–470. https://doi.org/10.3390/pharmaceutics7040438.

Anderson, A., Davis, J., 2017. Nanostructures for Drug Delivery. Elsevier,, pp. 183–206. https://doi.org/10.1016/B978-0-323-46143-6.00005-1.

Arias, J., Loez-Viota, M., Lopez-Viota, J., Delgado, A.V., 2009. Development of iron/ethylcellulose (core/shell) nanoparticles loaded with diclofenac sodium for arthritis treatment. Int. J. Pharm. 382, 270–276.

Barna, B.P., Huizar, I., Malur, A., McPeek, M., Marshall, I., Jacob, M., Dobbs, L., Kavuru, M.S., Thomassen, M.J., 2013. Carbon nanotube-induced pulmonary granulomatous disease: twist1 and alveolar macrophage M1 activation. Int. J. Mol. Sci. 14, 23858–23871. https://doi.org/10.3390/ijms141223858.

Bhavsar, M.D., Amiji, M.M., 2007. Gastrointestinal distribution and in vivo gene transfection studies with nanoparticles-in-microsphere oral system (NiMOS). J. Control Release 119, 339–348. https://doi.org/10.1016/j.jconrel.2007.03.006.

Bilyy, R., Bila, G., Vishchur, O., Vovk, V., Herrmann, M., 2020. Neutrophils as main players of immune response towards nondegradable nanoparticles. Nanomaterials 10, 1273. https://doi.org/10.3390/nano10071273.

Bryant, H.C., Sergatskov, D.A., Lovato, D., LAdolphi, N., Larson, R.S., Flynn, E.R., 2007. Magnetic needles and superparamagnetic cells. Phys. Med. Biol. 52, 4009–4025. https://doi.org/10.1088/0031-9155/52/14/001.

Cairns, R., Papandreou, I., Denko, N., 2006. Overcoming physiologic barriers to cancer treatment by molecularly targeting the tumor microenvironment. Mol. Cancer Res. 4, 61–70. https://doi.org/10.1158/1541-7786.MCR-06-0002.

Cebecauer, M., Hof, M., Amaro, M., 2017. Impact of GM1 on membrane-mediated aggregation/oligomerization of β-Amyloid: unifying view. Biophys. J. 113, 1194–1199. https://doi.org/10.1016/j.bpj.2017.03.009.

Chiricozzi, E., Pomè, D.Y., Maggioni, M., Di Biase, E., Parravicini, C., Palazzolo, L., Loberto, N., Eberini, I., Sonnino, S., 2017. Role of the GM1 ganglioside oligosaccharide portion in the TrkA-dependent neurite sprouting in neuroblastoma cells. J. Neurochem. 143, 645–659. https://doi.org/10.1111/jnc.14146.

Choi, H.S., Liu, W., Misra, P., Tanaka, E., Zimmer, J.P., Ipe, B.I., Bawendi, M.G., Frangioni, J.V., 2007. Renal clearance of quantum dots. Nat. Biotechnol. 25, 1165–1170. https://doi.org/10.1038/nbt1340.

Chueh, Ch-Ch, Chen, Ch-I., Su, Y.-A., Konnerth, H., Gu, Y.-J., Kung, Ch-W., Wu, K.C.-W., 2019. Harnessing MOF materials in photovoltaic devices: recent advances, challenges, and perspectives. J. Mater. Chem. A 7, 17079–17095. https://doi.org/10.1039/C9TA03595H.

Decuzzi, P., Godin, B., Tanaka, T., Lee, S.Y., Chiappini, C., Liu, X., Ferrari, M., 2010. Size and shape effects in the biodistribution of intravascularly injected particles. J. Control Release 141, 320–327. https://doi.org/10.1016/j.jconrel.2009.10.014.

Din, F., Aman, W., Ullah, I., Qureshi, O.S., Mustapha, O., Shafique, S., Zeb, A., 2017. Effective use of nanocarriers as drug delivery systems for the treatment of selected tumors. Int. J. Nanomed. 12, 7291–7309. https://doi.org/10.2147/IJN.S146315.

Doustkhah, E., Lin, J., Rostamnia, S., Len, C., Luque, R., Luo, X., Bando, Y., Wu, K.C.-W., Kim, J., Yamauchi, Y., Ide, Y., 2019. Development of sulfonic-acid-functionalized mesoporous materials: synthesis and catalytic applications. Chem. Eur. J. 25, 1614–1635. https://doi.org/10.1002/chem.201802183.

El-Boubbou, K., 2018. Magnetic iron oxide nanoparticles as drug carriers: clinical relevance. Nanomedicine 13, 953–971. https://doi.org/10.2217/nnm-2017-0336.

Forster, J.C., Harriss-Phillips, W.M., Douglass, M.J.J., Bezak, E., 2017. A review of the development of tumor vasculature and its effects on the tumor microenvironment. Hypoxia 5, 21–32. https://doi.org/10.2147/HP.S133231.

Gambardella, C., Mesaric, T., Milivojevic, T., Sepcic, K., Gallus, L., Carbone, S., Ferrando, S., Faimali, M., 2014. Effects of selected metal oxide nanoparticles on Artemia salina larvae: evaluation of mortality and behavioural and biochemical responses. Environ. Monit. Assess. 186, 4249–4259. https://doi.org/10.1007/s10661-014-3695-8.

Garbarino, V.R., Orr, M.E., Rodriguez, K.A., Buffenstein, R., 2015. Mechanisms of oxidative stress resistance in the brain: lessons learned from hypoxia tolerant extremophilic vertebrates. Arch. Biochem. Biophys. 576, 8–16. https://doi.org/10.1016/j.abb.2015.01.029.

Hamilton Jr, R.F., Buford, M., Xiang, C., Wu, N., Holian, A., 2012. NLRP3 infl ammasome activation in murine alveolar macrophages and related lung pathology is associated with MWCNT nickel contamination. Inhal. Toxicol. 24, 995–1008. https://doi.org/10.3109/08958378.2012.745633.

Hautot, D., Pankhurst, Q.A., Khan, N., Dobson, J., 2003. Preliminary evaluation of nanoscale biogenic magnetite in Alzheimer's disease brain tissue. Proc. Biol. Sci. 270, 62–64. https://doi.org/10.1098/rsbl.2003.0012.

Honda, K., Casadesus, G., Petersen, R.B., Perry, G., Smith, M.A., 2004. Oxidative stress and redox-active iron in Alzheimer's disease. Ann. N.Y. Acad. Sci. 1012, 179–182. https://doi.org/10.1196/annals.1306.015.

Huang, H.S., Hainfield, J.F., 2013. Intravenous magnetic nanoparticle cancer hyperthermia. Int. J. Nanomed. 8, 2521–2532. https://doi.org/10.2147/IJN.S43770.

Konnerth, H., Matsagar, B.M., Chen, S.S., Prechtl, M.H.G., Shieh, F.-K., Wu, K.C.-W., 2020. Metal-organic framework (MOF)-derived catalysts for fine chemical production. Coord. Chem. Rev. 416, 213319 https://doi.org/10.1016/j.ccr.2020.213319.

Kramers, H.A., 1940. Brownian motion in a field of force and the diffusion model of chemical reactions. Physica 7, 284–304. https://doi.org/10.1016/S0031-8914(40)90098-2.

Lee, C.C., Chen, C.I., Liao, Y.-T., Wu, K.C.-W., Chueh, C.C., 2019. Enhancing efficiency and stability of photovoltaic cells by using perovskite/Zr-MOF heterojunction including bilayer and hybrid structures. Adv. Sci. 6, 1801715 https://doi.org/10.1002/advs.201801715.

Lee, D.-H., Hernandez, J.M.T., 2018. The newest generation of drug-eluting stents and beyond. Eur. Cardiol. 13, 54–59. https://doi.org/10.15420/ecr.2018:8:2.

Liao, Y.-T., Matsagar, B.M., Wu, K.C.-W., 2018. Metal–organic framework (MOF)-derived effective solid catalysts for valorization of lignocellulosic biomass. ACS Sustain. Chem. Eng. 6, 13628–13643. https://doi.org/10.1021/acssuschemeng.8b03683.

Liao, Y.-T., Van Chia, N., Ishiguro, N., Young, A.P., Tsung, C.K., Wu, K.C.-W., 2020. Engineering a homogeneous alloy-oxide interface derived from metal-organic frameworks for selective oxidation of 5-hydroxymethylfurfural to 2,5-furandicarboxylic acid. Appl. Catal. B: Environ. 270, 118805 https://doi.org/10.1016/j.apcatb.2020.118805.

Liu, J.-L., Fan, Y.-G., Yang, Z.-Sh, Wang, Z.-Yu, Guo, C., 2018. Iron and Alzheimer's disease: from pathogenesis to therapeutic implications. Front. Neurosci. 12, 632. https://doi.org/10.3389/fnins.2018.00632.

Liu, Z., Ruan, Y., Yue, W., Zhu, Z., Hartmann, T., Beyreuther, K., Zhang, D., 2006. GM1 up-regulates ubiquilin 1 expression in human neuroblastoma cells and rat cortical neurons. Neurosci. Lett. 407, 59–63. https://doi.org/10.1016/j.neulet.2006.08.005.

Lyndon, J.A., Boyd, B.J., Birbilis, N., 2014. Metallic implant drug/device combinations for controlled drug release in orthopaedic applications. J. Control Release 179, 63–75. https://doi.org/10.1016/j.jconrel.2014.01.026.

Marcu, A., Pop, S., Dumitrache, F., Mocanu, M., Niculit, C.M., Gherghiceanu, M., Lungu, C.P., Fleaca, C., Ianchis, R., Barbut, A., Grigoriu, C., Morjan, I., 2013. Magnetic iron oxide nanoparticles as drug delivery system in breast cancer. Appl. Surf. Sci. 281, 60–65. https://doi.org/10.1016/j.apsusc.2013.02.072.

McGinty, S., 2014. A decade of modelling drug release from arterial stents. Math. Biosci. 257, 80–90.
Meng, L., Jiang, A., Chen, R., Li, C.Z., Wang, L., Qu, Y., Wang, P., Zhao, Y., Chen, C., 2013. Inhibitory effects of multiwall carbon nanotubes with high iron impurity on viability and neuronal differentiation in cultured PC12 cells. Toxicology 313, 49–58. https://doi.org/10.1016/j.tox.2012.11.011.
Mura, S., Nicolas, J., Couvreur, P., 2013. Stimuli-responsive nanocarriers for drug delivery. Nat. Mater. 12, 991–1003. https://doi.org/10.1038/nmat3776.
Mustapić, M., Hossain, M.S., Horvat, J., Wagner, P., Mitchell, D.R.G., Kim, J.H., Alici, G., Nakayama, Y., Martinac, B., 2016. Controlled delivery of drugs adsorbed onto porous Fe_3O_4 structures by application of AC/DC magnetic fields. Microporous Mesoporous Mater. 226, 243–250. https://doi.org/10.1016/j.micromeso.2015.12.032.
Nagy, J.A., Chang, S.-H., Dvorak, A.M., Dvorak, H.F., 2009. Why are tumour blood vessels abnormal and why is it important to know? Br. J. Cancer 100, 865–869. https://doi.org/10.1038/sj.bjc.6604929.
Nakayama, Y., Mustapić, M., Ebrahimian, H., Wagner, P., Kim, J.H., Hossain, M.S., Horvat, J., Martinac, B., 2015. Magnetic nanoparticles for smart liposomes. Eur. Biophys. J. 44, 647–654. https://doi.org/10.1007/s00249-015-1059-0.
Özgür, M.E., Ulu, A., Balcıoğlu, S., Özcan, İ., Köytepe, S., Ateş, B., 2018. The toxicity assessment of iron oxide (Fe_3O_4) nanoparticles on physical and biochemical quality of rainbow trout spermatozoon. Toxics 6, 62. https://doi.org/10.3390/toxics6040062.
Patra, J.K., Das, G., Fraceto, L.F., Campos, E.V.R., Rodriguez-Torres, M.P., Acosta-Torres, L.S., Diaz-Torres, L.A., Grillo, R., Swamy, M.K., Sharma, S., Habtemariam, S., Shin, H.-S., 2018. Nano based drug delivery systems: recent developments and future prospects. J. Nanobiotechnol. 16, 71. https://doi.org/10.1186/s12951-018-0392-8.
Peng, Q., Huo, D., Li, H., Zhang, B., Li, Y., Liang, A., Wang, H., Yu, Q., Li, M., 2018. ROS-independent toxicity of Fe_3O_4 nanoparticles to yeast cells: Involvement of mitochondrial dysfunction. Chem. -Biol. Interact. 287, 20–26. https://doi.org/10.1016/j.cbi.2018.03.012.
Pouponneau, P., Leroux, J.-C., Martel, S., 2009. Magnetic nanoparticles encapsulated into biodegradable microparticles steered with an upgraded magnetic resonance imaging system for tumor chemoembolization. Biomaterials 30, 6327–6332. https://doi.org/10.1016/j.biomaterials.2009.08.005.
Prausnitz, M.R., Langer, R., 2008. Transdermal drug delivery. Nat. Biotechnol. 26, 1261–1268. https://doi.org/10.1038/nbt.1504.
Primo, F.L., Macaroff, P.P., Lacava, Z.G.M., Azevedo, R.B., Morais, P.C., Tedesco, A.C., 2007. Binding and photophysical studies of biocompatible magnetic fluid in biological medium and development of magnetic nanoemulsion: a new candidate for cancer treatment. J. Magn. Magn. Mater. 310, 2838–2840. https://doi.org/10.1016/j.jmmm.2006.11.062.
Qi, M., Zhang, K., Li, S., Wu, J., Pham-Huy, C., Diao, X., Xiao, D., He, H., 2016. Superparamagnetic Fe_3O_4 nanoparticles: synthesis by a solvothermal process and functionalization for a magnetic targeted curcumin delivery system. New J. Chem. 40, 4480–4491. https://doi.org/10.1039/c5nj02441b.
Qu, C., Wang, L., He, J., Tan, J., Liu, W., Zhang, S., Zhang, C., Wang, Z., Jiao, S., Liu, S., Jiang, G., 2012. Carbon nanotubes provoke infl ammation by inducing the pro-infl ammatory genes IL-1beta and IL-6. Gene 493, 9–12. https://doi.org/10.1016/j.gene.2011.11.046.
Ramaswamy, B., Kulkarni, S.D., Villar, P.S., Smith, R.S., Eberly, C., Araneda, R.C., Depireux, D.A., Shapiro, B., 2015. Movement of magnetic nanoparticles in brain tissue: mechanisms and safety. Nanomedicine 11, 1821–1829. https://doi.org/10.1016/j.nano.2015.06.003.
Reshmi, G., Mohan Kumar, P., Malathi, M., 2009. Preparation, characterization and dielectric studies on carbonyl iron/cellulose acetate hydrogen phthalate core/shell nanoparticles for drug delivery applications. Int. J. Pharm. 365, 131–135. https://doi.org/10.1016/j.ijpharm.2008.08.006.
Šegota, S., Baranović, G., Mustapić, M., Strassera, V., Domazet Jurašin, D., Crnolatac, I., Hossain, M.S., Dutour Sikirić, M., 2019. The role of spin-phonon coupling in enhanced desorption kinetics of antioxidant flavonols from magnetic nanoparticles aggregates. J. Magn. Magn. Mater. 490, 165530 https://doi.org/10.1016/j.jmmm.2019.165530.
Shen, L., Li, B., Qiao, Y., 2018. Fe_3O_4 nanoparticles in targeted drug/gene delivery systems. Materials 11, 324. https://doi.org/10.3390/ma11020324.
Simon-Deckers, A., Gouget, B., Mayne-L'Hermite, M., Herlin-Boime, N., Reynaud, C., Carriere, M., 2008. In vitro investigation of oxide toxicity and intracellular accumulation in A549 human pneumocytes. Toxicology 253, 137–146. https://doi.org/10.1016/j.tox.2008.09.007.
Singh, N., Jenkins, G.J., Asadi, R., Doak, S.H., 2010. Potential toxicity of superparamagnetic iron oxide nanoparticles (SPION). Nano Rev. 1, 5358. https://doi.org/10.3402/nano.v1i0.5358.
Soppimath, K.S., Aminabhavi, T.M., Kulkarni, A.R., Rudzinski, W.E., 2001. Biodegradable polymeric nanoparticles as drug delivery devices. J. Control Release 70, 1–20. https://doi.org/10.1016/S0168-3659(00)00339-4.
Tashima, Y., Oe, R., Lee, S., Sugihara, G., Chambers, E.J., Takahashi, M., Yamada, T., 2004. The effect of cholesterol and monosialoganglioside (GM1) on the release and aggregation of amyloid beta-peptide from liposomes prepared from brain membrane-like lipids. J. Biol. Chem. 279, 17587–17595. https://doi.org/10.1074/jbc.m308622200.
Traitel, T., Goldbart, R., Kost, J., 2008. Smart polymers for responsive drug-delivery systems. J. Biomater. Sci. Polym. Ed. 19, 755–767. https://doi.org/10.1163/156856208784522065.
Tucek, J., Zboril, R., Petridis, D., 2006. Maghemite nanoparticles by view of Mossbauer spectroscopy. J. Nanosci. Nanotechnol. 6, 926–947. https://doi.org/10.1166/jnn.2006.183.
Valentini, X., Rugira, P., Frau, A., Tagliatti, V., Conotte, R., Laurent, S., Colet, J.-M., Nonclercq, D., 2019. Hepatic and renal toxicity induced by TiO_2 nanoparticles in rats: a morphological and metabonomic study. J. Toxicol. 19, 2019. https://doi.org/10.1155/2019/5767012.
Vangijzegem, T., Stanicki, D., Laurent, S., 2019. Magnetic iron oxide nanoparticles for drug delivery: applications and characteristics. Expert Opin. Drug Deliv. 16, 69–78. https://doi.org/10.1080/17425247.2019.1554647.
Wang, J., Xu, Y., Ding, B., Chang, Z., Zhang, X., Yamauchi, Y., Wu, K.C.-W., 2018. Confined self-assembly in two-dimensional interlayer space: monolayered mesoporous carbon nanosheets with in-plane orderly arranged mesopores and a highly graphitized framework, 2729-2729 Angew. Chem. Int. Ed. 57. https://doi.org/10.1002/anie.201801793.
Wang, J.-Y., Zhuang, Q.-Q., Zhu, L.-B., Zhu, H., Li, T., Li, R., Chen, S.-F., Huang, C.-P., Zhang, X., Zhu, J.-H., 2016. Meta-analysis of brain iron levels of Parkinson's disease patients determined by postmortem and MRI measurements. Sci. Rep. 6, 36669. https://doi.org/10.1038/srep36669.
Warheit, D.B., Donner, E.M., 2010. Rationale of genotoxicity testing of nanomaterials: regulatory requirements and appropriateness of available OECD test guidelines. Nanotoxicology 4, 409–413. https://doi.org/10.3109/17435390.2010.485704.
Wei, W., Wang, Z., 2018. Investigation of magnetic nanoparticle motion under a gradient magnetic field by an electromagnet. J. Nanomater. 5, 6246917 https://doi.org/10.1155/2018/6246917.
Wiemann, M., Vennemann, A., Blaske, F., Sperling, M., Kars, U., 2017. Silver nanoparticles in the lung: toxic effects and focal accumulation of silver in remote organs. Nanomaterials 7, 441. https://doi.org/10.3390/nano7120441.
Wu, J., Ding, T., Sun, J., 2013. Neurotoxic potential of iron oxide nanoparticles in the rat brain striatum and hippocampus. Neurotoxicology 34, 243–253. https://doi.org/10.1016/j.neuro.2012.09.006.
Xia, T., Hamilton, R.F., Bonner, J.C., Crandall, E.D., Elder, A., Fazlollahi, F., Girtsman, T. A., Kim, K., Mitra, S., Ntim, S.A., Orr, G., Tagmount, M., Taylor, A.J., Telesca, D., Tolic, A., Vulpe, C.D., Walker, A.J., Wang, X., Witzmann, F.A., Wu, N., Xie, Y., Zink, J.I., Nel, A., Holian, A., 2013. Interlaboratory evaluation of in vitro cytotoxicity and infl ammatory responses to engineered nanomaterials: the NIEHS Nano GO Consortium. Environ. Health Perspect. 121, 683–690. https://doi.org/10.1289/ehp.1306561.
Liu, P.F., Liu, D., Cai, C., Chen, X., Zhou, Y., Wu, L., Sun, Y., Dai, H., Kong, X., Xie, Y., 2016. Size-dependent cytotoxicity of Fe_3O_4 nanoparticles induced by biphasic regulation of oxidative stress in different human hepatoma cells. Int. J. Nanomed. 11, 3557–3570. https://doi.org/10.2147/IJN.S105575.
Xue, Y., Wu, J., Sun, J., 2012. Four types of inorganic nanoparticles stimulate the inflammatory reaction in brain microglia and damage neurons in vitro. Toxicol. Lett. 214, 91–98. https://doi.org/10.1016/j.toxlet.2012.08.009.
Yanagisawa, K., Ihara, Y., 1998. GM1 ganglioside-bound amyloid beta-protein in Alzheimer's disease brain. Neurobiol. Aging 19, 65–67. https://doi.org/10.1016/s0197-4580(98)00032-3.
Zhang, W.E., Prausnitz, M.R., Edwards, A.U., 2004. Model of transient drug diffusion across cornea. J. Control Release 99, 241–258. https://doi.org/10.1016/j.jconrel.2004.07.001.